DEUTSCHES ELEKTRONEN-SYNCHROTRON DESY

DESY SR-82-06
May 1982

RESONANT PHOTOEMISSION OF ATOMIC Mn

by

R. Bruhn, E. Schmidt, H. Schröder and B. Sonntag

II. Institut für Experimentalphysik der Universität Hamburg
and Deutsches Elektronen-Synchrotron DESY, Hamburg

NOTKESTRASSE 85 · 2 HAMBURG 52

To be sure that your preprints are promptly included in the
HIGH ENERGY PHYSICS INDEX ,
send them to the following address (if possible by air mail) :

DESY
Bibliothek
Notkestrasse 85
2 Hamburg 52
Germany

DESY SR-82-06
May 1982

Resonant Photoemission of Atomic Mn

R. Bruhn, E. Schmidt, H. Schröder and B. Sonntag

II. Institut für Experimentalphysik der Universität Hamburg
and Deutsches Elektronen-Synchrotron DESY, 2Hamburg 52, Germany

The photoemission of atomic Mn has been obtained in the photon energy range 40 eV to 56 eV. The strong coupling of the 3p and 3d excitations leads to a resonant enhancement of the $3d^5(^6S)\ 4s$, $3d^5\ (^4X)\ 4s$, $3d^4\ (^5D)\ 4s^2$ and $3d^4\ (^5D)\ 4s\ nl$ photoemission lines above the 3p threshold.

Accepted for publication in Physics Letters A

At the 3p threshold the absorption spectrum of atomic Mn is dominated by a strong asymmetric absorption band. This band is due to the interference between the discrete $3p^6\ 3d^5\ 4s^2 \rightarrow 3p^5\ 3d^6\ 4s^2$ transitions and the continuum transitions $3p^6\ 3d^5\ 4s^2 \rightarrow 3p^6\ 3d^4\ 4s^2\ \varepsilon f$ (1,2). In order to be able to discriminate between the different channels contributing to the absorption and to gain more insight into the coupling of these channels, the photoemission of atomic Mn has been investigated.
For this purpose the synchrotron radiation emitted by the storage ring DORIS was monochromatized with a new toroidal grating monochromator. The monochromatic photon beam (bandwidth = 0,2 eV) was focussed onto the interaction zone where it crossed a beam of atomic Mn emanating from a resistively heated high temperature furnace. The kinetic energy of electrons emerging from the interaction zone was determined by a cylindrical mirror analyzer (angular acceptance 0,8% of 4π, energy resolution ΔE = 0,8 % of the pass energy). Only electrons emitted at the magic angle of 54° 44' relative to the polarization vector of the incoming light were accepted by the analyzer. This eliminates the asymmetry of the photoelectron angular distribution (3) and allows for a direct determination of partial cross-sections. All photoemission spectra were normalized to the incoming photon flux and corrected for the energy dependent dispersion of the electron analyzer. Since the density of Mn atoms in the interaction zone was not determined, only relative cross-sections are given. Details of the experimental set-up will be presented elsewhere (4).

In Fig. 1 the photoemission spectrum of atomic Mn taken at 50,0 eV photon energy is shown. There is a dominant line corresponding to the $3d^4\ (^5D)\ 4s^2\ ^5D$ state of Mn II accompanied by a series of weaker lines. Our assignment, in part based on tabulated atomic energy values (5) is summarized in Table 1. The partial cross-sections for the emission of the outer 4s and 3d electrons are strongly influenced by the coupling to the 3p excitations. This can be directly read off from Fig. 2 in which a series of photoemission spectra taken at different photon energies are given together with the absorption spectrum. The main photoemission line (No. 6) is suppressed at the 3p-threshold and strongly enhanced in the region of $3p^6\ 3d^5\ 4s^2\ ^6S \rightarrow 3p^5\ 3d^6\ 4s^2\ ^6P$ transitions, which contribute most to the dominant absorption band (1,2). Except for the marked increase at $h\omega$ = 55.4 eV where transitions to $3p^5\ 3d^5\ 4s^2\ nl$ ($n > 3$) contribute to the absorption,

the intensities of the lines 1 - 4 show a similar dependence on the photon energy. This supports our tentative assignment of these lines to $3d^4$ (^{5}D) 4s nl states of Mn II. The intensity versus photon energy of these lines resembles the absorption spectrum. The Fano type profile (6) clearly manifests the interference between the 3p and 3d excitations. In contrast the strength of the lines 7 - 10, assigned to the $3d^5$ (^{4}X) $4s^5$ X states of Mn II is similar at 48 eV and at 50,5 eV. Also the asymmetry of the intensity versus photon energy curve is much less pronounced. The corresponding curves for the photoemission lines assigned to the $3d^5$ (^{6}S) 4s ^{5,7}S states of Mn II can be approximated by the superposition of two Lorentzian lines positioned at 48 eV and 50 eV. These lines are driven by the $3p^5\ 3d^6\ 4s^2 \rightarrow 3p^6\ 3d^5\ 4s\ \varepsilon l$ decay. They are symmetric, since they are only weakly influenced by interference with the $3p^6\ 3d^5\ 4s^2 \rightarrow 3p^6\ 3d^5\ 4s\ \varepsilon l$ excitation due to the small cross-section for the 4s excitation.

In order to put our discussion of the 3p - 3d intershell coupling on a firmer basis, we will compare the variation of the intensity with photon energy for the most prominent lines, i.e. the lines assigned to the $3d^4$ (^{5}D) $4s^2\ ^5$D and the $3d^5$ (^{6}S) 4s ^{5,7} S states of Mn II, to the results of a model calculation. The model is based on the extension of Fano's theory (6) to the case of many discrete states interacting with many continua by Davis and Feldkamp (7,8). The model, schematically depicted below, takes the interaction between the discrete states Φ_1, Φ_2 and the continua $\psi_{1\varepsilon}$, $\psi_{2\varepsilon}$ and the spin-orbit coupling of the 3p core into account.

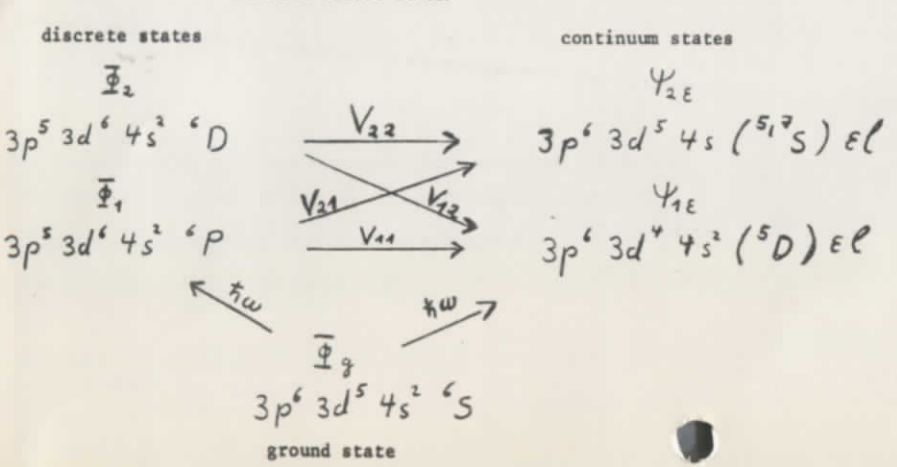

For the autoionisation matrix elements $V_{ki} = \langle\psi_{k\varepsilon} / H / \Phi_i\rangle$ the following relations hold: $V_{12} = 0$ due to symmetry (2), $V_{11} > V_{22}$ due to three instead of two electrons having the same principal quantum number. In our model the matrix elements V_{ki}, the matrix element $\lambda = \langle\Phi_1/H/\Phi_2\rangle$ proportional to the spin-orbit interaction of the 3p core and the asymmetry parameter q (3,6) have been used as parameters.

Direct optical excitations from the ground state to Φ_2 and $\psi_{2\varepsilon}$ have been neglected. The experimental data and the results of the model calculation are presented in Fig. 3. It is obvious that the model well describes the characteristic features of the experimental spectra. The parameters given in Fig. 3 are in reasonable agreement with those reported in the literature (2). Transitions to other states (e.g. $3p^5\ 3d^6$ (^{4}X) $4s^2$) autoionizing into $3p^6\ 3d^4\ 4s^2$ (^{5}D) εl are probably responsible for the deviations between 50 eV and 53 eV. Marked discrepancies between the calculated curves and the experimental results show up at photon energies below 49 eV. These are in part due to the limited experimental resolution which results in a considerable broadening of the ^{6}D line. Due to this and due to the neglect of the interaction with the $3d^5$ (^{4}X) 4s εl continua the model overestimates the coupling between the $3p^5\ 3d^6\ 4s^2\ ^6$D state and the $3p^6\ 3d^5$ 4s (^{5,7}S) εl continuum. Furthermore, it is clear from the nonzero intensity of the ^{5,7} S photoemission lines below 47 eV that the $3d^5\ 4s^2 \rightarrow 3d^5$ 4s εp cross-section is not zero as assumed in our model. The transition to the $^4P_{5/2}$ line at 48,5 eV (see absorption spectrum in Fig. 2) is reflected in the $3p^6$ ed^4 $4s^2$ (^{5}D) channel. This proves that transitions to $3p^5\ 3d^6\ 4s^2\ ^4$X states are also coupled to this channel. These transitions may in part also be responsible for the enhancement of the $3d^5$ (^{4}X) 4s ^{5}X photoemission lines.

Acknowledgment

The authors profited very much from many discussions with L.C. Davis and from his formulation of the model.

REFERENCES

1. R. Bruhn, B. Sonntag and H.W. Wolff, Phys. Lett. 69A (1978) 9

2. L.C. Davis and L.A. Feldkamp, Phys. Rev. A17 (1978) 2012

3. A.F. Starace, Theory of Atomic Photoionization, in: Handbuch der Physik, Vol. 31, ed. by W. Mehlhorn, Springer Verlag, Berlin to be published.

4. R. Bruhn, E. Schmidt, H. Schröder, and B. Sonntag, Proc. Int. Conf. on X-ray and VUV Synchrotron Radiation Instrumentation, Hamburg 1982. Special volume of Nuclear Instruments and Methods (to be published).

5. Ch. Corliss and J. Sugar, J. of Phys. and Chem., Reference Data 6, (1977) 1253.

6. U. Fano, Phys. Rev. 124 (1961) 1866.

7. L.C. Davis and L.A. Feldkamp, Phys. Rev. B15 (1977) 2961.

8. L.C. Davis and L.A. Feldkamp, Phys. Rev. B23 (1981) 6239.

Table 1

Experimental binding energies E_B of the states of Mn II giving rise to the photoemission lines in Fig. 1. The tabulated binding energy of the $3d^5\ (^6s)\ 4s\ ^7s_3$ state(s) has been used as reference.

Line	E_β (eV)	State of Mn II
1	25.1 ± 0.2	$3d^4\ (^5D)\ 4s\ nl$
2	24.2 ± 0.2	$3d^4\ (^5D)\ 4s\ nl$
3	20.8 ± 0.2	$3d^4\ (^5D)\ 4s\ 4p\ ^5P$ tent.
4	20.6 ± 0.2	$3d^4\ (^5D)\ 4s\ 4p\ ^5F$ "
5	15.4 -17.7	$3d^5\ (^4X)\ 4p\ ^5X$ "
6	14.2 ± 0.15	$3d^4\ (^5D)\ 4s^2\ ^5D$
7	12.8 ± 0.1	$3d^5\ (^4F)\ 4s\ ^5F$
8	11.5 ± 0.1	$3d^5\ (^4D)\ 4s\ ^5D$
9	11.2 ± 0.1	$3d^5\ (^4P)\ 4s\ ^5P$
10	10.8 ± 0.1	$3d^5\ (^4G)\ 4s\ ^5G$
11	9.3 ± 0.1	$3d^6\ (^5D)\ ^5D$
12	8.6 ± 0.05	$3d^5\ (^6s)\ 4s\ ^5S_2$
13	7.44	$3d^5\ (^6s)\ 4s\ ^7S_3$ ref.

Figure Captions

Fig. 1 Photoemission spectrum of atomic Mn taken at $\hbar\omega$ = 50 eV.

Fig. 2 Photoemission spectra of atomic Mn taken at various photon energies (lower part). The photon energies at which the photoemission spectra were recorded are given on the energy scale of the absorption spectrum of atomic Mn (upper part).

Fig. 3 Experimentally determined intensity of the $3d^4\ 4s^2\ ^5D$ (·) and the sum of the $3d^5\ 4s\ ^{5,7}S$ (x) photoemission lines as a function of the photon energy. The results of the model calculation are given by the solid lines.

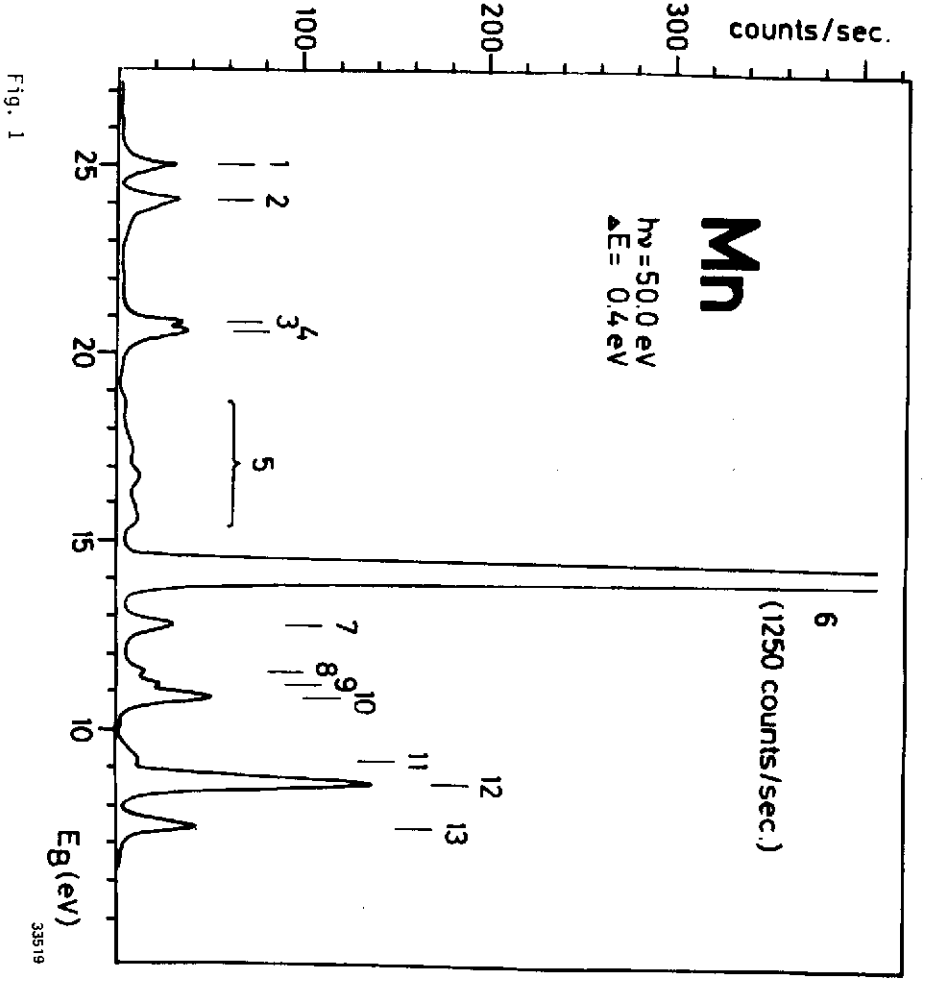

Fig. 1

Fig. 2

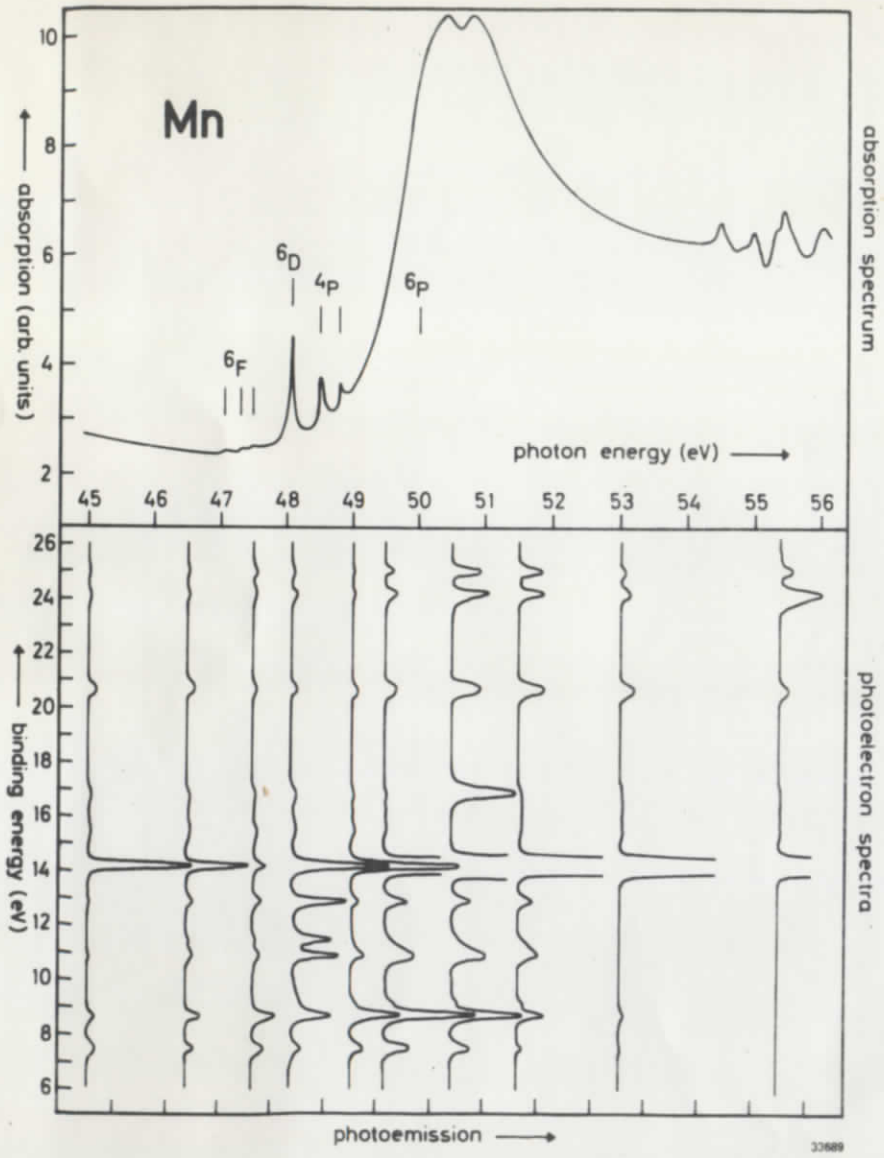
Mn
absorption (arb. units)
absorption spectrum
6F
6D
4P
6P
photon energy (eV)
45 46 47 48 49 50 51 52 53 54 55 56
binding energy (eV)
photoelectron spectra
photoemission
33689

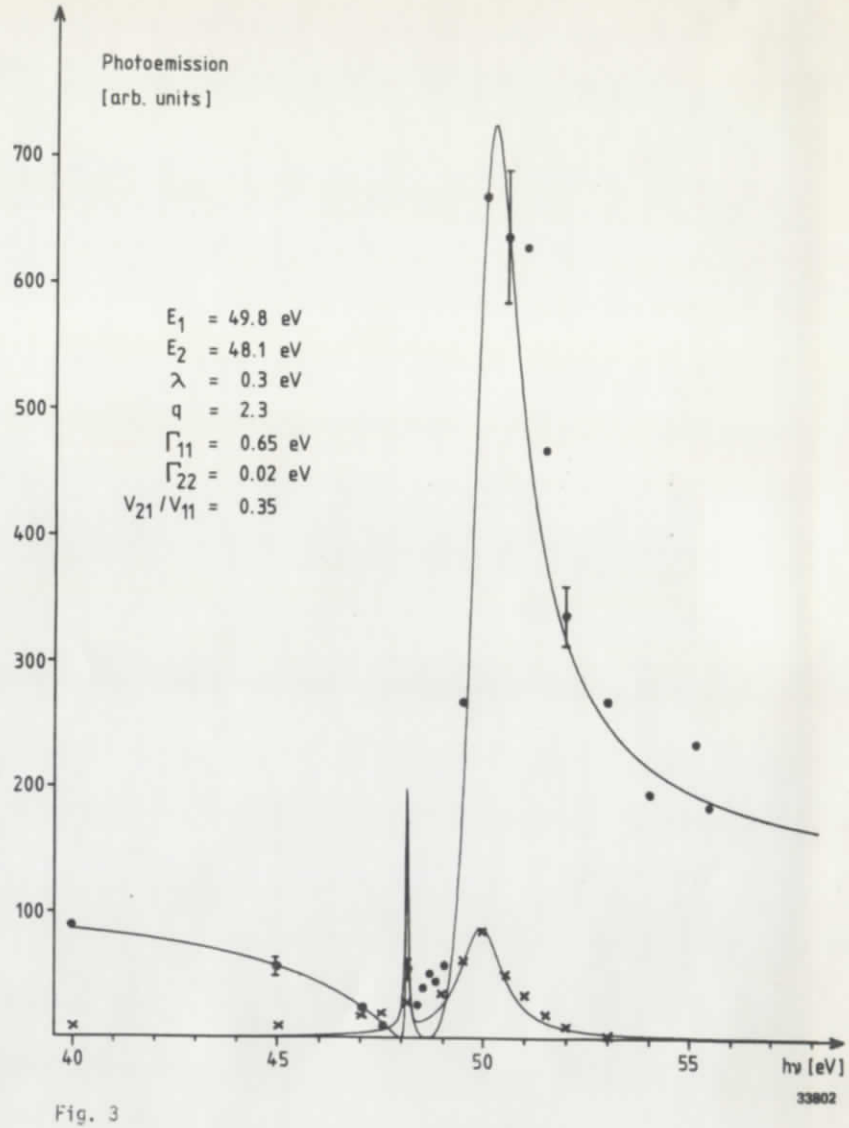
Photoemission
[arb. units]
E1 = 49.8 eV
E2 = 48.1 eV
λ = 0.3 eV
q = 2.3
Γ11 = 0.65 eV
Γ22 = 0.02 eV
V21 / V11 = 0.35
700
600
500
400
300
200
100
40
45
50
55
hν [eV]
33802

Fig. 3